SCIENTIFIC REPORTS

OPEN

SUBJECT AREAS:
TECHNIQUES AND INSTRUMENTATION
METEORITICS
GEOCHEMISTRY

Received
9 December 2013

Accepted
1 May 2014

Published
27 May 2014

Correspondence and requests for materials should be addressed to K.T. (terada@ess.sci.osaka-u.ac.jp)

A new X-ray fluorescence spectroscopy for extraterrestrial materials using a muon beam

K. Terada[1], K. Ninomiya[1], T. Osawa[2], S. Tachibana[3], Y. Miyake[4,5], M. K. Kubo[6], N. Kawamura[4,5], W. Higemoto[7], A. Tsuchiyama[8], M. Ebihara[9] & M. Uesugi[10]

[1]Graduate School of Science, Osaka University, [2]Quantum Beam Science Directorate, Japan Atomic Energy Agency, [3]Graduate School of Science, Hokkaido University, [4]Muon Science Section, Materials and Life Science Division, J-PARC Center, [5]Muon Science Laboratory, IMSS, High Energy Accelerator Research Organization, [6]Graduate School of Science, International Christian University, [7]Advanced Science Research Center, Japan Atomic Energy Agency, [8]Graduate School of Science, Kyoto University, [9]Graduate School of Science and Engineering, Tokyo Metropolitan University, [10]JAXA Space Exploration Center, Japan Aerospace Exploration Agency.

The recent development of the intense pulsed muon source at J-PARC MUSE, Japan Proton Accelerator Research Complex/MUon Science Establishment (10^6 s^{-1} for a momentum of 60 MeV/c), enabled us to pioneer a new frontier in analytical sciences. Here, we report a non-destructive elemental analysis using μ^- capture. Controlling muon momentum from 32.5 to 57.5 MeV/c, we successfully demonstrate a depth-profile analysis of light elements (B, C, N, and O) from several mm-thick layered materials and non-destructive bulk analyses of meteorites containing organic materials. Muon beam analysis, enabling a bulk analysis of light to heavy elements without severe radioactivation, is a unique analytical method complementary to other non-destructive analyses. Furthermore, this technology can be used as a powerful tool to identify the content and distribution of organic components in future asteroidal return samples.

The muon is a lepton with a mass of 105.7 MeV/c^2, approximately 200 times heavier than the electron. The interaction between muons and materials has been used in various fields of research. Muon spin rotation, relaxation, and resonance (μSR) use polarised positive muons as sensitive magnetic microprobes with short-range interactions with materials. Muon tomography uses the highly transmissive nature of muons to image low-density regions of materials. Recent studies on tomographic imaging with cosmic ray muons have succeeded in imaging the density structure of volcanoes[1–3].

Muons entering materials lose their kinetic energy with less effective bremsstrahlung than electrons due to their heavier mass; they can also penetrate much deeper into materials than electrons. The penetration depth of muons depends on the density of the target material and the initial muon momentum. Negative muons are captured by atoms to form muonic atoms at the stopping depths. In a muonic atom, cascade transition of the trapped muon from higher to lower energy states occurs with the emission of characteristic muonic X-rays. As muons have an orbit closer to the atomic nucleus than electrons owing to its ~200 times heavier mass, the characteristic muonic X-ray has an energy ~200 times higher than that associated with electron transition (more than several ten keV even if the muon is captured in light elements). The muonic X-rays are thus intense enough to pass through the target material from the much deeper interior than the characteristic X-rays of electron transitions, thereby suggesting that muonic X-rays from muonic atoms can be applicable to non-destructive elemental analyses of the deep interior of materials, which cannot be performed with X-ray fluorescence spectroscopy or electron probe microanalysis.

In 1971, Rosen[4] noted the great availability of muon beam analysis and proposed its application in the chemical analysis of tissues, as muon beam analysis would cause less damage to the host organism than neutron activation analyses. Muonic atom spectroscopy has been developed over the past four decades[5–7] as a non-destructive analytical method; however, for a real application, one had to wait for an intense muon source. The intense pulsed muon source, J-PARC MUSE (Japan Proton Accelerator Research Complex, MUon Science Establishment), was constructed and succeeded in providing a decay muon rate of 10^6 s^{-1} for a momentum of 60 MeV/c in November 2009, which is the most intense pulsed muon beam in the world[8,9]. Although J-PARC was damaged by a magnitude 9 earthquake and a subsequent tsunami on 11 March 2011 ("Higashi-Nippon Dai-Shinsai[10–12]"), it was successfully revived in February 2012[13].

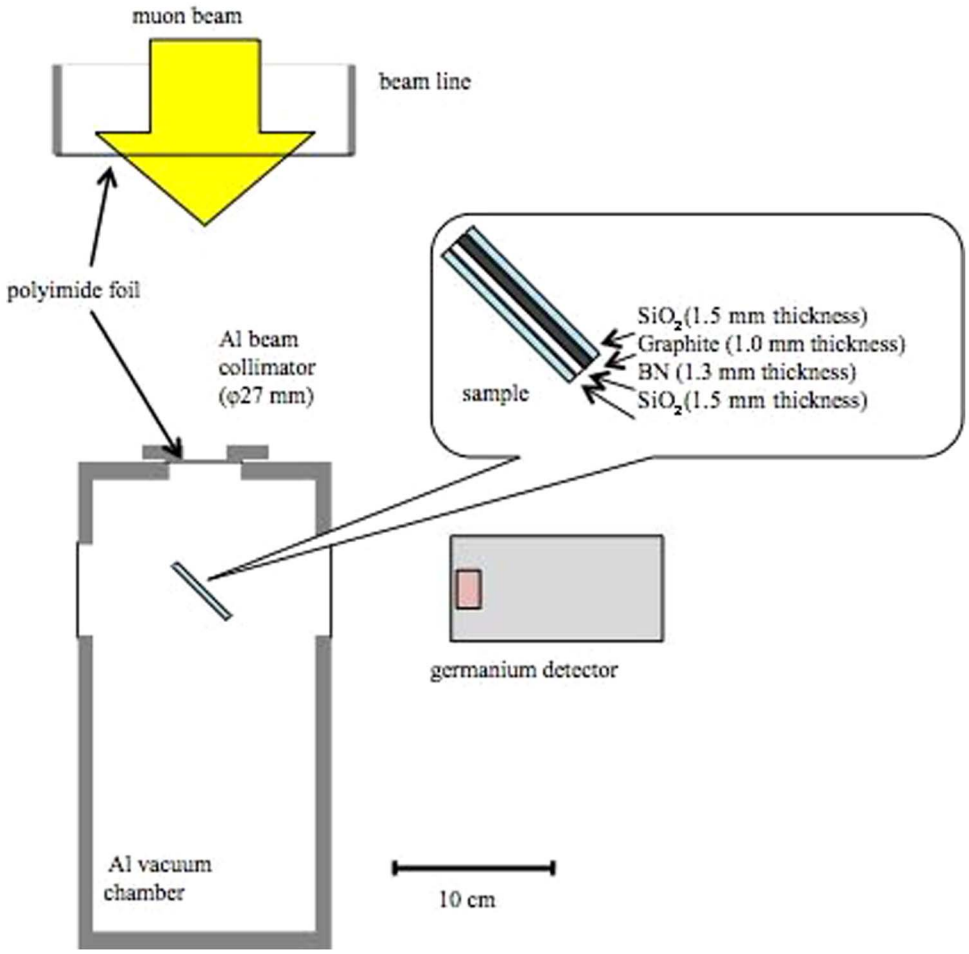

Figure 1 | Geometry of the depth profile analysis. A four-layered sample (SiO_2-graphite-BN-SiO_2) and a Ge detector were oriented at 45 and 90 degrees to the negative muon beam, respectively, in an aluminium vacuum chamber with a polyimide window. The muon beam was collimated to 4-2.5 cm in diameter. The sample was supported by a holder made of aluminium foil.

We report a feasibility study of the non-destructive muon beam chemical analysis of light elements (C, N, O and B) from millimetre- to centimetre-sized samples, which are difficult to analyse via neutron activation analysis, using the D2 muon beam line at J-PARC MUSE. Moreover, the degree of radioactivation due to muon irradiation is much less than that of neutron activation analysis, thereby allowing various applications. A potential useful application of this technique is, for instance, non-destructive analyses of light elements in extraterrestrial samples, particularly those obtained in sample return missions. Two sample return missions, Hayabusa-2[14] and OSIRIS-REx[15], will aim for C-type asteroids, for which reflectance spectra resemble those of carbonaceous chondrites containing organic materials. Millimetre- to centimetre-sized asteroidal surface samples will be returned in the 2020s[14–15], and the non-destructive analyses of light elements will prove to be a powerful analytical tool to determine the contents and/or distribution of organic materials, which may have been prebiotic building blocks of life, in pebble-sized noble samples.

Results

The depth profiling of light elements from a layered sample. The muon beam analysis of a four-layered sample consisting of SiO_2 glass, graphite (C), boron nitride (BN), and SiO_2 glass was generated to obtain a depth profile of light elements. The sample is held by an aluminium holder in an aluminium vacuum chamber with a beam-entrance window composed of polyimide foil.

The negative muon beam was collimated to approximately 2.7 cm in diameter and focused on the sample surface (50 mm × 75 mm), which was oriented at 45 degrees to the beam (Fig. 1). Adjusting the muon momentum from 32.5 MeV/c to 57.5 MeV/c, muonic X-rays from the sample were measured by a Ge detector. The accumulation time of X-ray signals was 3–4 hours for each muon momentum. Figure 2 shows the observed X-ray spectra for the different momentum of incident muon beams. The energies of muonic X-rays listed in Engfer et al.[16] were used for peak identification. Note that the peaks at 66 and 89 keV represent Al signals from the sample holder and vacuum chamber. At the momentum of 32.5 MeV/c, the μSi-Lα (76 keV) and μO-Kα (133 keV) signals were detected with the background μAl-Lα (66 keV). The peaks of μSi-Lα and μO-Kα were also confirmed at the momentum of 37.5 and 40.0 MeV/c, although they disappeared at the momentum 42.5 MeV/c, where the μC-Kα (75 keV) signal was clearly observed. As the μC-Kα peak should come from the second graphite layer, these observations suggest that the muon beam penetrated through the first SiO_2 glass layer and into the depth of >2 mm of the sample at the momentum of 42.5 MeV/c. The findings also demonstrate that the characteristic muonic X-ray of carbon was emitted from a depth of >2 mm through the overlying SiO_2 glass layer without significant self-absorption and emission of muonic X-rays of Si and O. At the momentum of 50.0 MeV/c, the μC-Kα peak disappeared and only μB-Kα (52 keV) and μN-Kα (102 keV) signals from the third layer (boron nitride) were detected through the overlying SiO_2 and graphite layers. Finally, at the momentum of 57.5 MeV/c, the peaks of μB-Kα and μN-Kα disap-

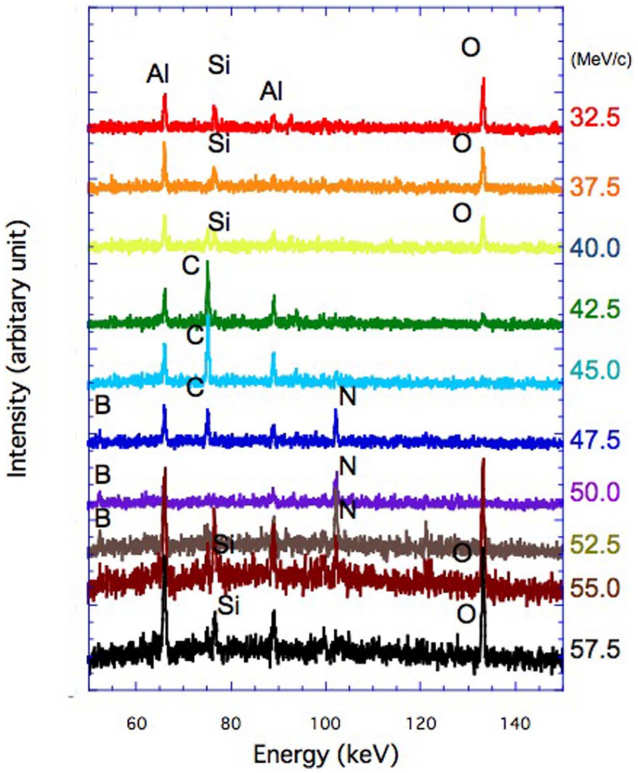

Figure 2 | Muonic X-ray energy spectra from the four-layered sample. Muonic X-ray intensities (y-axis) are shown in arbitrary units with offset to compare the spectra obtained with different muon momenta (32.5–57.5 MeV/c). The peaks at 66 and 89 keV are attributed to Al used for a sample holder and the vacuum chamber. The peaks of μSi-Kα and μO-Kα were detected from the first SiO_2 glass layer at the muon momentum of 32.5–40.0 MeV/c. The muonic X-ray of C (μC-Kα) from the graphite layer and those of B and N from the BN layer were detected at the momenta of 42.5–47.5 and 47.5–52.5 MeV/c, respectively. The peaks of μSi-Kα and μO-Kα were detected again at the muon momentum of 55.0–57.5 MeV/c from the bottom SiO_2 glass layer through the three overlying layers.

peared, and the μSi-Lα (76 keV) and μO-Kα (133 keV) signals were again detected. This clearly shows that the muon beam penetrated into the depth of >5.3 mm through the layered sample, and the μSi-Lα (76 keV) and μO-Kα (133 keV) from muonic atoms in the fourth SiO_2 glass layer were emitted through the overlying layers.

The intensities of muonic X-ray signals of B, C, N, O, and Si with 1σ uncertainties from counting statistics of X-rays are plotted against the muon momentum, as displayed in Figure 3. Because the contributions of μAl-Kα from the vacuum chamber and the sample holder should be almost constant irrespective of the muon momentum, the intensity of each peak of muonic X-ray was normalised to that of μAl-Lα. The stopping depth of muons in the sample at a given momentum was estimated based on the Bethe-Bloch formula, which is generally used to calculate the energy loss of charged particles travelling in a medium, using the density and thickness of each layer. The depths corresponding to the boundaries of sample layers (indicated by arrows) are consistent with the change in muonic X-ray signals from the sample.

The self–absorption effects on μSi-Lα (76 keV) and μO-Kα (133 keV) at the depth of ~7 mm are estimated to be 20% of the densities and thicknesses of overlying layers, which are consistent with slightly weak peak intensities of μSi-Lα (76 keV) and μO-Kα (133 keV) at the momenta of 55 and 57.5 MeV/c compared with those of the first layers (32.5 and 37.5 MeV/c) (Fig. 3).

The current depth estimate should have a ~10% uncertainty largely due to the momentum range of the incident muon beam.

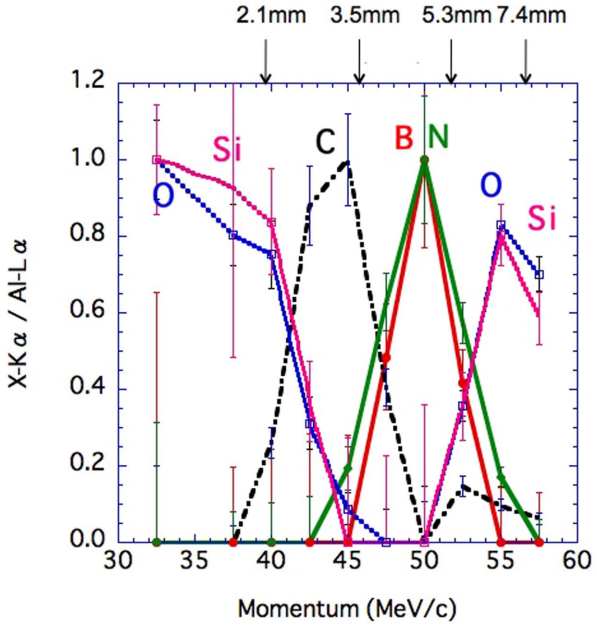

Figure 3 | The depth-profile of the four-layered sample. The muonic X-ray intensities of B, C, N, O, and Si from the layered sample are plotted against the muon momentum. The muonic X-ray intensity of each element is normalised to the intensity of μAl-Kα at each momentum and to its maximum count along the depth profile. Analytical uncertainties (1σ) are estimated from the counting statistics of X-ray counts because the contributions of uncertainties in X-ray detection efficiency are much smaller than those of counting statistics (typically less than 5%). The stopping depth of muons at a given momentum is estimated from the Bethe-Bloch formula, and the expected layer boundaries are indicated by arrows.

Although there are further developments in experimental techniques, such as momentum filtering of the incident muon beam and a position-sensitive detector, we currently conclude that the non-destructive depth profile of light elements was successfully obtained up to ~7 mm in depth with a depth resolution of sub-mm. This result is hardly possible with other analytical techniques such as neutron activation analysis, X-ray fluorescence spectroscopy and electron probe microanalysis. Furthermore, muon beam analysis displays significant potential for the analysis of light element distributions within millimetre- to centimetre-sized samples.

Elemental analysis of meteorite samples. Muonic beam analysis was applied to primitive meteorites called chondrites. Chondrites have never been melted and remain physical aggregates of various components that formed in the early solar system prior to planet formation. Carbonaceous chondrites are one of the various chemical groups of chondrites, some of which contain abundant water as hydrated minerals and organic materials[17]. They record the long evolutionary history of the solar system and prebiotic organic reservoirs. Thus, future asteroidal sample return missions (Hayabusa-2 and OSIRIS-REx) plan to sample such materials from asteroids without terrestrial contamination and with geologic contexts[14,15].

In this study, we carried out a non-destructive muon analysis of chips of carbonaceous chondrites, Murchison and Allende. The Murchison meteorite contains a copious amount of diverse extraterrestrial organic materials, while the Allende meteorite contains less carbon than the Murchison meteorite.

The negative muon beam, collimated to approximately 4 cm in diameter, irradiated to a ~5-mm-thick Murchison disk with the exposed surface area of ~5 cm × ~10 cm. The meteorite disk and the Ge detector were oriented at 45 and 90 degrees to the negative

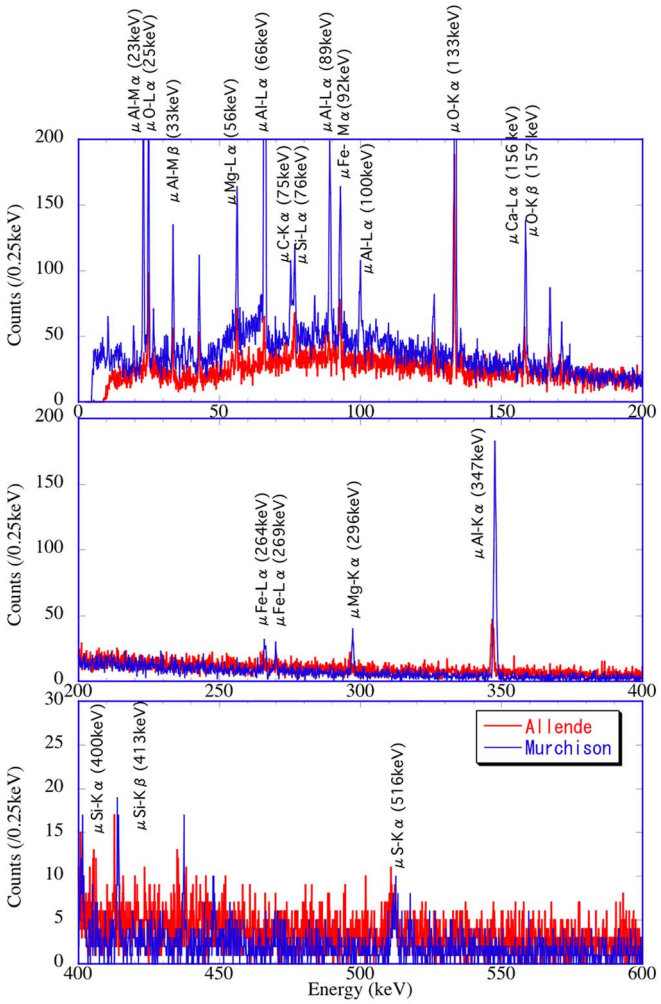

Figure 4 | Muonic X-ray energy spectra from carbonaceous chondrites: Murchison and Allende meteorites. Fluorescent X-rays of Mg, C, Si, Fe, Ca, and S were detected from the Murchison meteorite (blue), while those of Mg, Si, Fe, K, and Ca were detected from the Allende meteorite (red). The peaks of Al includes signals from the vacuum chamber and/or the sample holder. The peak of μC-Kα (75 keV) was detected from the Murchison meteorite,

muon beam, respectively, in the same manner shown in Fig. 1. Aluminium foil was used to hang the sample inside the chamber. The exposure time was approximately 13 hours, and the momentum of the incident muon beam was set at 16 MeV/c, corresponding to the penetration depth of ~70 μm. For Allende meteorite analysis, the muon beam was collimated to approximately 2.7 cm in diameter at the sample surface of 50 mm × 75 mm. The sample was also hung with less amounts of Al foil than for the Murchison meteorite to reduce the background signal of Al. The exposure time was approximately 10 hours, and the incident muon momentum was set at 34 MeV/c (the penetration depth of ~1 mm).

Table 1 | Characteristic muonic X-ray counts from carbonaceous chondrites, the Murchison and Allende meteorites

Characteristic X-ray	Energy (keV)	Murchison	Allende
Ca-Mα	55	n.d.	53 ± 23
Mg-Lα	56	896 ± 66	183 ± 23
Al-Lα	66	10796 ± 130	136 ± 30
C-Kα	75	626 ± 52	6 ± 27
Si-Lα	76	824 ± 58	175 ± 32
Fe-Mα	94	1310 ± 63	265 ± 39
O-Kα	133	4785 ± 111	800 ± 38
K-Lα	140	n.d.	94 ± 27
Ca-Lα	156	213 ± 41	83 ± 28
Al-Kα	346	9542 ± 100	359 ± 27
S-Kα	516	121 ± 33	11 ± 9

n.d.: Not detected.

Fluorescent X-rays of Mg, C, Si, Fe, Ca, and S were detected from the Murchison meteorite, while X-rays of Mg, Si, Fe, K, and Ca were detected from the Allende meteorite (Fig. 4; Table 1). Clear signals of Al were also obtained, although they should include background signals from the vacuum chamber and/or the sample holder and are therefore excluded from further discussion. Taking the emission probabilities of Kα and Lα fluorescent lines and the energy-dependence of Ge detector efficiency into account[16], the captured muon counts for C, Si, Mg and O and for S and Fe were obtained from the integrated intensities of the Kα and Lα fluorescent lines, respectively. In Fig. 5, the captured muon counts normalised to that of Mg are plotted against the Mg-normalised weight concentrations of elementsin the Murchison and Allende meteorites. The captured muon count is roughly proportional to the weight concentration, with the exception of O, which has a high muon capture probability due to its high electronegativity[18]. The linear correlation in Fig. 5 indicates that the muon capture rate of an element is largely controlled by its concentration in a meteorite sample and neither self-absorption of muonic X-rays with different energies nor difference in chemical bonding have significant effects on muon capture.

Elements with concentrations of more than 1 weight percent were detected in this study. The detection limit of ~1 weight percent is attributed to the inefficient detection of muonic X-rays with a single

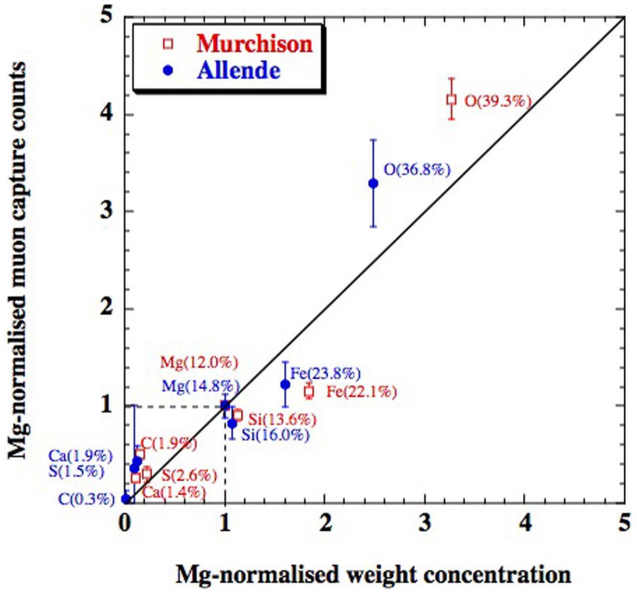

Figure 5 | Correlation between the elemental concentration and the captured muon counts. The captured muon counts by each element, normalised to those of Mg, are plotted against the Mg-normalised weight concentrations of elements in meteorite samples[33] after correction of the energy-dependent detector efficiency and the emission probabilities of the Kα and Lα fluorescent lines. The captured muon counts correspond to the characteristic muonic X-ray counts. Error bars show analytical uncertainties (1σ) estimated from the counting statistics of X-ray counts.

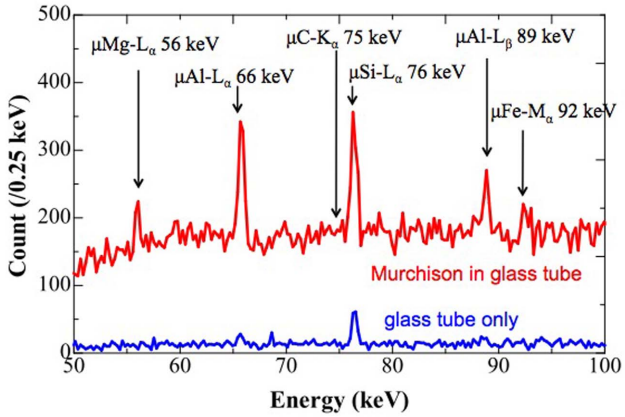

Figure 6 | Muonic X-ray spectra from the powdered Murchison meteorite in an SiO_2 glass tube. A clear signal of Mg and a marginally resolved signal of Fe from the sample were detected through the 1-mm thick SiO_2 glass wall. The intense signal of Si originated from the SiO_2 glass tube. The muon beam momentum was set at 37 MeV/c, and the exposure time was 24 hours.

Ge detector. Only 1% of the total emitted muonic X-rays can be detected by the Ge detector (5 cm in diameter) with the current experimental set-up, which will be significantly improved, i.e., with multiple detectors covering a much larger solid angle.

We also attempted to measure much smaller amounts of meteorite samples inside glass tubes to simulate non-destructive analyses of future return samples. Sealing extraterrestrial samples inside glass tubes was originally planned for samples from the asteroid Itokawa. Although Itokawa particles were not sealed in glass tubes due to their small sizes[19–21], sealing in a glass tube is one of the effective ways to avoid terrestrial contamination of organic materials and volatiles and thus could be used in future sample return missions.

Powdered Murchison meteorite (610 mg) was placed in a 5-cm-long SiO_2 glass tube, in which the inner and outer diameters were 4 mm and 6 mm, respectively. The muon beam collimated to approximately 2.5 cm in diameter, and the apparent cross section of the sample was 4 mm × 25 mm. After exposure of the muon beam with the momentum of 37 MeV/c for approximately 24 hours, clear signals of Mg and marginally resolved signals of Fe were detected through the 1-mm thick glass wall (Fig. 6). Although O and Si are the major elements of rock samples, muonic X-rays of O and Si were emitted from the SiO_2 glass tube as well, which cannot be distinguished from the sample signals. Although further developments in analytical techniques are required, such as detector setting and collimation of the incident muon beam, our first attempt to non-destructively measure an extraterrestrial sample inside a glass tube succeeded with the detection of Mg and Fe.

Discussion

This study demonstrates that muon beam analysis is feasible for the non-destructive elemental analysis of light elements in extraterrestrial samples. This technique is complementary to other non-destructive analytical techniques, such as synchrotron X-ray microtomography and synchrotron X-ray diffraction, both of which have been used for preliminary examination of Itokawa particles[19,20] to obtain structural and mineralogical information. Neutron activation analysis was also applied to Itokawa particles for bulk elemental analyses, including trace elements[21]. X-ray photoelectron spectroscopy (XPS)[22,23] and X-ray absorption spectroscopy (XAS)[24] at synchrotron facilities have been used to identify the chemical bonding of elements. Synchrotron X-ray absorption near-edge structure (XANES) spectroscopy has been used to identify chemical bonding and functional groups in cometary organic matter sampled from the comet 81P/Wild 2 by the Stardust spacecraft[25]. Nuclear reaction analysis (NRA) can be used to determine the contents and distribution of C, N, and O in minerals[26]. The recent development of direct tomography with chemical bond contrast using synchrotron X-ray has made it possible to make a 3D map of the chemical bonding of light elements in a cm-sized sample with a spatial resolution of ~100 μm[27]. These techniques have not only benefits but also disadvantages, including severe radioactivation of samples, limitations in sample size and analytical area and/or depth, limited number of measurable elements, and difficulties in bulk analysis. Muon beam analysis is capable of performing a bulk analysis of light to heavy elements at one time without severe radioactivation and is thus a unique and complementary analytical method.

J-PARC MUSE plans to increase the power of the proton beam, of which irradiation of a graphite target produces the muon beam, up to 1 MW[13]. The muon beam intensity will increase to ~10^7 count/s (i.e., ten times larger than the current beam), which will yield a significant improvement in the counting statistics of muonic X-ray detection. The counting statistics will also be improved by development of the detection system (e.g., multiple Ge detectors covering a larger solid angle[28]). With a more effective detector setting, the chemical structure states of Fe may be determined because the muonic X-ray structure, such as μKα/μKβ ratios, could depend on chemical structure state[29,30]. Iron is present as metallic Fe-Ni, iron sulfides, FeO in silicates and chondrites, and its oxidation state has long been used as one of the classification criteria of chondrites. Moreover, this method has a future prospect of non-destructive three-dimensional mapping of multi-elements using, for instance, a position-sensitive detector with a large cross-section, such as Compton Camera[31,32], and may represent the dawn of another "eye" after the proposition of muon radiography by Rosen[4] more than forty years ago.

Methods

The muon science facility (MUSE) is located in the Materials and Life Science Facility (MLF), a facility that includes both neutron and muon science programs, at the Japan Proton Accelerator Research Complex (J-PARC) in Tokai, Japan. MUSE currently

has two beam lines to extract surface muons and decay muons from the muon source target into the experimental halls[13]. Negative decay muons (5–120 MeV/c), which are obtained via the in-flight decay of μ^+/μ^- confined by a strong longitudinal magnetic field of a superconducting solenoid magnet, were used in this study. Since November 26, 2010, the proton beam power from the Rapid Cycling Synchrotron has been steadily increased up to 220 kW, consequently delivering approximately 10^6 count/s of decay muon beam (μ^+ and μ^-), until the earthquake on March 11, 2011. Although MUSE was seriously damaged from so-called 'Higashi-Nippon Dai-Shinsai', it recovered in six months and restarted operations for external users in February 2012. As a top priority analysis, this study was carried out in February 2012 and January 2013. The muon beam line at J-PARC/MUSE is now open for external users through a peer-reviewed proposal system (twice a year) as other analytical techniques in synchrotron facilities.

1. Tanaka, H. K. M. *et al.* Imaging the conduit size of the dome with cosmic-ray muons: The structure beneath Showa-Shinzan Lava Dome, Japan. *Geophys. Res. Lett.* **34**, L22311, doi:10.1029/2007GL031389 (2007).
2. Tanaka, H. K. M., Uchida, T., Tanaka, M. & Shinohara, H. Cosmic-ray muon imaging of magma in a conduit: Degassing process of Satsuma-Iwojima Volcano, Japan. *Geophys. Res. Lett.* **36**, L01304, doi:10.1029/2008GL036451 (2009).
3. Tanaka, H. K. M., Kusagaya, T. & Shinohara, H. Radiographic visualization of magma dynamics in an erupting volcano. *Nat. Comm.* **5**, doi:10.1038/ncomms4381 (2014).
4. Rosen, L. Relevance of Particle Accelerators to National Goals. *Science* **173**, 490–497 (1971).
5. Daniel, H. Application of X-ray from negative muons. *Nucl. Instrum. Methods Phys. Res., B* **3**, 65–70 (1984).
6. Kubo, M. K. *et al.* Non-destructive elemental depth-profiling with muonic X-rays. *J. Radioanal. Nucl. Chem.* **278**, 777–781 (2008).
7. Ninomiya, K. *et al.* Development of Nondestructive and Quantitative Elemental Analysis Method Using Calibration Curve between Muonic X-ray Intensity and Elemental Composition in Bronze. *Bull. Chem. Soc. Jpn.* **85**, 228–230 (2012).
8. Cyranoski, D. Beamline bonanza for Japanese researchers. *Nature* **456**, 426–427 (2008).
9. Miyake, Y. *et al.* Birth of an intense pulsed muon source, J-PARC MUSE J-PARC muon source, MUSE. *Nucl. Instrum. Methods Phys. Res., A* **600**, 22–24 (2009).
10. Fuyuno, I. Quake shakes Japan's science. *Nature* **471**, 420–420 (2011).
11. Normile, D. Japan's research facilities down but not out. *Science* **331**, 1509–1509 (2011).
12. Normile, D. Picking up the pieces at ravaged Tohoku University. *Science* **333**, 153–155 (2011).
13. Miyake, Y. *et al.* J-PARC Muon Facility, MUSE. *Phys. Procedia* **30**, 46–49 (2012).
14. Tachibana, S. *et al.* Hayabusa-2: Sample return from a near-Earth C-type asteroid, 1999 JU_3. *Mineral. Mag.* **78**, in press (2014).
15. Lauretta, D. S. and the OSIRIS-REx team Cosmochemistry in support of OSIRIS-REx mission objectives. *Mineral. Mag.* **78**, in press (2014).
16. Engfer, R., Schneuwly, H., Vuilleumier, J. L., Walter, H. K. & Zehnder, A. Charge-distribution parameter, isotope shifts, isomer shift, and magnetic hyperfine constants from muonic atoms. *At. Data Nucl. Data Table* **14**, 509–597 (1974).
17. Scott, E. R. D. & Krot, A. N. Chondrite and their components. in: *Treatise on Geochemistry vol. 1.,* 143–200 (Elsevier, Oxford and San Diego, 2005).
18. Schneuwly, H., Pokrovsky, V. I. & Ponomarev, L. I. On coulomb capture ratios of negative measons in chemical compounds. *Nucl. Phys. A* **312**, 419–426 (1978).
19. Nakamura, T. *et al.* Itokawa dust particles: A direct link between S-type asteroids and ordinary chondrites. *Science* **333**, 1113–1116 (2011).
20. Tsuchiyama, A. *et al.* Three-dimensional structure of Hayabusa samples: Origin and evolution of Itokawa regolith. *Science* **333**, 1125–1128 (2011).
21. Ebihara, M. *et al.* Neutron activation analysis of a particle returned from asteroid Itokawa. *Science* **333**, 1119–1121 (2011).
22. Osawa, T. Kr and Xe implanted on the surfaces of Mo, Hf, W, Re, Au and platinum group elements. *Nucl. Instrum. Methods Phys. Res., B* **274**, 93–99 (2012).
23. Horiba, K. *et al.* Scanning photoelectron microscope for nanoscale three-dimensional spatial-resolved electron spectroscopy for chemical analysis. *Rev. Sci. Instrum.* **82**, doi: 10.1063/1.3657156 (2011).
24. Osawa, T. Quantitative estimation methods for concentrations and layer thicknesses of elements using edge-jump ratios of x-ray absorption spectra. *Anal. Sci.* **26**, 281–284 (2010).
25. Cody, G. D. *et al.* Quantitative organic and light-element analysis of comet 81P/Wild 2 particles using C-, N-, and O- XANES. *Meteor. Planet. Sci.* **43**, 353–365 (2008).
26. Varela, M. E., Bonnin-Mosbah, M., Kurat, G. & Gallien, J. P. Nitrogen microanalysis of glass inclusions I chondritic olivines by nuclear reaction. *Geochim. Cosmochim. Acta* **67**, 1247–1257 (2003).
27. Huotari, S., Pylkkänen, T., Verbeni, R., Monaco, G. & Hämäläinen, K. Direct tomography with chemical-bond contrast. *Nat. Mater.* **10**, 489–493 (2011).
28. Lee, I. Y., Deleplanque, M. A. & Vetter, K. Developments in large gamma-ray detector arrays, *Rep. Prog. Phys.* **66**, 1095–1144 (2003).
29. Schneuwly, H. *et al.* Capture of negative muons in cubic and hexagonal structures of carbon and boron nitride. *Phys. Rev. A* **27**, 950–960 (1983).
30. Daniel, H., Hartmann, F. J. & Naumann, R. A. Solid-state effects on Coulomb capture and x-ray cascade of negative muons. *Phys. Rev. A* **59**, 3343–3348 (1999).
31. Domingo-Pardo, C. A new technique for 3D gamma-ray imaging: Conceptual study of a 3D camera. *Nucl. Instrum. Methods Phys. Res., A* **675**, 123–132 (2012).
32. Odaka, K. *et al.* High-resolution Compton cameras based on Si/CdTe double-sided strip detectors. *Nucl. Instrum. Methods Phys. Res., A* **695**, 179–183 (2012).
33. Jarosewich, E. Chemical analyses of meteorites: A compilation of stony and iron meteorite analyses. *Meteoritics* **25**, 323–337 (1990).

Acknowledgments

We are grateful to all the staff of J-PARC MUSE for their technical assistance. This study is partly supported by Grant-in-Aids for Scientific Research (22224010) (KT, ST, and ME) and for Young Scientists (A) (25706032) (TO), and Promotion for Young Research Talent and Network (Northern Advancement Center for Science & Technology) (ST).

Author contributions

K.T. and K.N. organised the entire research project and contributed to all aspects of this study. Y.M., M.K.K., N.K. and W.H. contributed to the development and set-up of the muon beam line at J-PARC MUSE, and T.O., S.T. and M.K.K. performed sample analyses with muon beam. A.T., M.E. and M.U. contributed to the discussion on the experimental set-up and comparison with other non-destructive techniques. K.T. and S.T. wrote the manuscript with T.O. and N.K. and all authors reviewed the manuscript.

Additional information

Competing financial interests: The authors declare no competing financial interests.

How to cite this article: Terada, K. *et al.* A new X-ray fluorescence spectroscopy for extraterrestrial materials using a muon beam. *Sci. Rep.* **4**, 5072; DOI:10.1038/srep05072 (2014).